ELSEVIER

Polymer 43 (2002) 1829–1834

polymer

www.elsevier.com/locate/polymer

Solid-state organization of poly(methylmethacrylate)–poly(methylphenylsiloxane) based interpenetrating networks

L. Brachais[a], F. Lauprêtre[a,*], J.-R. Caille[a,1], D. Teyssié[b], S. Boileau[a]

[a]*Laboratoire de Recherche sur les Polymères, UMR 7581-CNRS, 2 rue Henri Dunant, 94320 Thiais, France*
[b]*Laboratoire des Polymères et Matériaux Electroactifs, Université de Cergy-Pontoise, 5 mail Gay-Lussac, 95031 Neuville sur Oise Cedex, France*

Received 30 July 2001; received in revised form 27 September 2001; accepted 2 November 2001

Abstract

Three interpenetrating networks based on polymethylphenylsiloxane (PMPS) and polymethylmethacrylate (PMMA) with different compositions were prepared. They were investigated using differential scanning calorimetry (DSC) and high-resolution solid-state ^{13}C NMR techniques, in order to study the heterogeneous character of the domains involved in these materials at the nanoscopic scale. DSC observed broad glass transitions of the PMPS chains. ^{13}C cross-polarization (CP) experiments clearly showed that the aromatic PMPS carbons have a rate of CP which is composition dependent, indicating that PMPS and PMMA chains are interpenetrating at a very low spatial scale. These results were supported by $T_{1\rho}(^1H)$ and ^{13}C line width measurements as a function of temperature. Moreover, $T_{1\rho}(^1H)$ measurements indicated that PMMA chains are rather homogeneously distributed whereas PMPS chains belong either to interpenetrating domains or to PMPS-rich domains.

Keywords: Interpenetrating polymer networks; Poly(methylphenylsiloxane); Poly(methylmethacrylate)

1. Introduction

Synthesizing interpenetrating polymer networks (IPNs) is a well-known way to force the compatibility of immiscible polymers. Such materials are of particular interest when they are made from two components which exhibit highly different properties [1–3]. In this respect, IPNs based on polymethylphenylsiloxane (PMPS) and polymethylmethacrylate (PMMA), which have been prepared recently [4], can be considered as typical examples: at room temperature, neat PMPS is a rubbery polymer, whereas atactic PMMA is well below its glass transition temperature.

Since the network properties are expected to be highly dependent on the quality of the interpenetration, it is very important to investigate the interpenetrating character of IPNs. In the case of highly different components like PMPS and PMMA, several techniques can be used. Each technique characterizes the domain sizes in the material under study with its own spatial scale. For example, transparency of the samples is a well-known criterion for the interpenetrating character of networks. In a transparent material, the domain sizes must be of the order of or smaller than the visible wavelengths, i.e. a few hundreds of nanometers. Larger domains should result in opaque samples.

Differential scanning calorimetry (DSC), dynamic mechanical analysis (DMA) and, more general, techniques which detect the glass transition temperature, T_g, can give information on the compatibility of polymers at a very low spatial scale of the order of a few nanometers [5–8]. Immiscible polymer blends are known to exhibit several T_gs corresponding to each neat component T_g. In compatible polymer blends, only one T_g is observed, the value of which is located between the T_gs of the homopolymers and depends on the blend composition [9]. However, miscible polymer blends are very rare since they need appropriate solubility parameters to achieve an intimate mixing. It is interesting to use this general approach to study the interpenetrating character of IPNs for which the idea is to force the compatibility of polymers, whatever the solubility parameters [10]. In the particular case of PMPS/PMMA based IPNs, T_gs of both components are highly different (−30 °C [11] and 90 °C, respectively) and DSC should prove to be an interesting method to investigate a phase separation at a spatial scale of a few nanometers.

Several solid-state NMR parameters are available to characterize the solid-state organization of multi-component

* Corresponding author. Tel.: +33-1-4978-1286; fax: +33-1-4978-1208.
E-mail address: francoise.laupretre@glvt-cnrs.fr (F. Lauprêtre).
[1] Present address: CERM, Université de Liège, B6, Sart-Tilman, 4000 Liège, Belgium.

0032-3861/02/$ - see front matter
PII: S0032-3861(01)00764-9

polymer systems [12,13]. Some parameters, such as the ^{13}C line widths, are sensitive to differences in the chain mobility between a neat homopolymer and an IPN component due to the changes in the intermolecular interactions. Other techniques based on the rises of ^{13}C magnetization in a cross-polarization (CP) experiment or on the measurements of ^{1}H spin–lattice relaxation times in the rotating frame, take advantage of the spin diffusion commonly observed in solids and thus probe the chain environment [14–23]. ^{13}C-detected $T_{1\rho}(^{1}H)$ measurements are a very powerful tool for monitoring the phase separated domains in immiscible polymer blends. In a homogeneous sample, all protons relax at about the same rate via spin diffusion [24]. In a blend, when the phase separated domains are larger than 1–2 nm, different proton relaxation rates may be observed. On the opposite, if carbon resonances associated to each homopolymer component exhibit the same $T_{1\rho}(^{1}H)$ value, then the efficiency of the spin diffusion during the few milliseconds of the spin–lattice relaxation in the rotating frame indicates that the material is homogeneous at the length scale of 1–2 nm. This criterion can be readily applied to investigate the chain environments of each IPN component.

For IPNs made of glassy and rubbery components, the CP experiments may be used to study the neighborhood of each component at a still shorter spatial scale of a few angstroms. The rate of the ^{13}C polarization rise in a CP experiment depends on the strength of the ^{1}H–^{1}H and ^{13}C–^{1}H dipolar interactions. Glassy materials result in a rapid rise of the observed ^{13}C intensities while rubbery materials exhibit a slower rise. Therefore, flexible chains have a faster CP rise when they are close to more rigid chains as it may occur in a glassy/rubbery IPN, than when they are close to other flexible chains as they are in the neat polymer.

The purpose of the present work is to characterize the interpenetration of three PMPS/PMMA based IPNs with different compositions. In this study, DSC and NMR experiments have been employed to probe the interpenetrating character at different length scales.

2. Experimental

2.1. IPN synthesis

Five samples including two homopolymer networks (PMMA and PMPS) and three interpenetrating networks with different compositions were prepared as described previously [4,25]. IPN synthesis was achieved using the in situ sequential method in which the first network is formed at low temperature in the presence of the components of the second polymer network, which is obtained at a higher temperature. In this strategy, the PMPS network was formed by condensation of the silanol end groups of the telechelic siloxane oligomers ($\bar{M}_n = 4300$) with a mixed crosslinking agent, such as trimethoxysilylpropylmethacrylate, at room temperature, with a catalytic amount of dibutyltindilaurate.

Table 1
Composition of the samples under study and glass transition temperatures, T_g, as determined by DSC

Sample	Composition (% w/w)		T_g (K)
	PMPS	PMMA	
PMPS	100	0	241
IPN75	75	25	241
IPN50	50	50	245
IPN25	25	75	244
PMMA	0	100	363

The polymethacrylate network was then obtained by free-radical polymerization performed at 70 °C with AIBN as an initiator and 5% of ethyleneglycol dimethacrylate (EGDMA) as a crosslinking agent. Code names and compositions of samples are reported in Table 1.

2.2. DSC analysis

Thermograms were recorded on a Perkin Elmer DSC7 calorimeter. Samples were first cooled down to 203 K and then heated up to 433 K at the rate of 20 K/min. All samples underwent this thermal treatment twice. Glass transition temperatures were measured at the intersection of the extrapolated base line at the low temperature end and the tangent to the curve at the inflexion point. They correspond to the onset of the glass transition phenomenon.

2.3. NMR experiments

High-resolution solid-state ^{13}C NMR spectra were obtained at 75 MHz on a Bruker ASX 300 spectrometer monitored with Bruker Xwin-NMR software. A variable temperature 4 mm magic angle spinning (MAS) probe head was used. For experiments performed below room temperature, a low temperature kit using liquid nitrogen evaporation was connected to the probe head. After cryogenic grinding, samples were packed in zirconia dioxyde rotors closed with borum nitride caps allowing variable temperature measurements. High-resolution spectra were obtained using the combined techniques of CP, dipolar decoupling (DD) and MAS [26]. Hartman-Hahn condition was set with a glycine sample. A 4.8 μs 90° ^{1}H pulse, corresponding to ^{13}C and ^{1}H magnetic field strengths of 50 kHz, was used with a spectral width of 33 kHz on the ^{13}C channel. Chemical shift calibrations were done using the glycine carbonyl carbon resonance at 176 ppm. For CP experiments, the best sensitivity was reached with a contact duration close to 1 ms. However, for experiments measuring the efficiency of CP as a function of the contact time, 16 spectra were recorded with different contact durations ranging from 0 up to 13 ms. All MAS experiments were recorded at the spinning frequency of 6500 Hz, leading to spectra with no residual sidebands, except for PMMA carbonyl carbon which exhibits a very broad chemical shift anisotropy.

Selective $T_{1\rho}(^{1}H)$ measurements were performed using a

spin-lock pulse sequence with a delayed contact time. In these experiments, 17 variable ^{1}H spin-lock delays from 1 up to 20 ms were used prior to CP. The signal intensities were then plotted as a function of the delay. The obtained curves were fitted using Igor-Pro software from Wave-Metrics. The $T_{1\rho}(^1\mathrm{H})$ decreases were fitted with an exponential function or with the sum of two exponential functions when necessary.

For line width experiments, 10 spectra were recorded for each sample at temperatures ranging from 250 to 333 K. Full medium-height line widths were then measured on Fourier transformed spectra.

3. Results

All synthesized samples were transparent indicating that there is no phase separation at the microscopic scale. Therefore, the domain sizes involved in all samples and, particularly in the IPNs, are smaller than a few hundreds of nanometers.

3.1. DSC

T_g values, as determined from DSC are reported in Table 1. Pure PMMA and PMPS networks have T_g values of 363 and 241 K, respectively. All three IPN samples exhibit a single broad glass transition. The onset of the glass transition observed in the three IPNs corresponds to the onset of the glass transition of the neat PMPS network. The only difference with the neat PMPS network is the width of the transition, which extends over 20–35° depending on the sample. The glass transition of the PMMA component is not detected by DSC in the IPNs under study.

3.2. NMR

As an example, the ^{13}C NMR spectrum of the IPN75 is shown in Fig. 1.

PMPS shows a high field signal around 0 ppm and several lines in the range 120–140 ppm assigned to the methyl group and aromatic carbons, respectively. PMMA exhibits five signals at 16 ppm (methyl group), 45 ppm (quaternary carbon), 51 ppm (methoxy group), 55 ppm (methylene group) and 177 ppm (carbonyl carbon). The different signals were readily assigned in the IPN spectrum since there are no overlaps between the lines of PMMA and those of PMPS and no significant chemical shift change with respect to the signals of the neat components.

Fig. 2 shows the measured intensities of PMPS protonated aromatic carbons as a function of the contact duration, t_{CP}, for the homopolymer PMPS network as well as for the three IPN samples at room temperature. As expected, the rubbery neat PMPS network exhibits a slow increase of carbon polarization since PMPS is far above its T_g. The maximum polarization transfer is reached for $t_{CP} = 11$ ms;

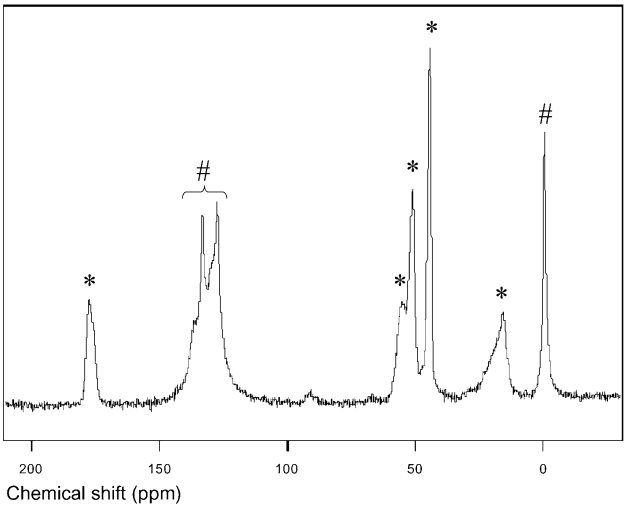

Fig. 1. 75 MHz ^{13}C CP–MAS NMR spectrum of IPN75. Lines characteristic of the PMPS or PMMA network are marked with (#) and (*) symbols, respectively.

at longer t_{CP}, the magnetization decay is governed by the $T_{1\rho}(^1\mathrm{H})$ relaxation. In the IPN samples, the PMPS aromatic carbons have a much faster polarization transfer. The time constants of the observed polarization rises are typical of glassy materials [12]. These results show that the presence of glassy PMMA in IPN modifies the PMPS phenyl group environment. They are a clear indication that at least a significant part of PMMA and PMPS units are within a distance to each other of a few Angstroms and therefore that the networks are interpenetrating at this low spatial scale. This conclusion is supported by the fact that the polarization rises are composition dependent and that the fastest polarization rise is obtained for the IPN25 sample which contains the largest amount of PMMA. As a matter of fact, this sample reaches its maximum polarization at

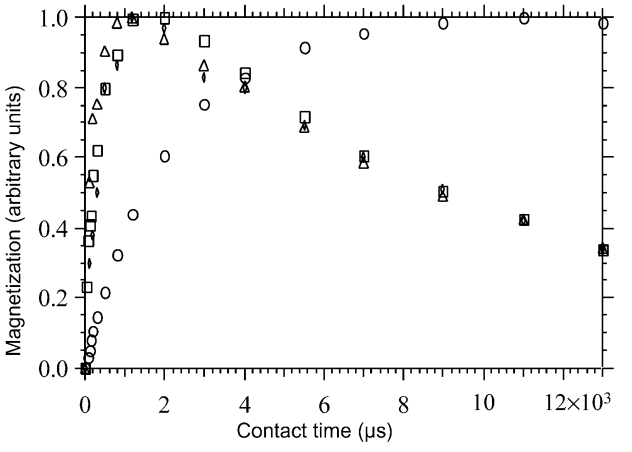

Fig. 2. Line intensity of aromatic PMPS carbons as a function of the contact time used during CP. ○ symbols represent the CP rise of the PMPS homopolymer network. □, △ and ◇ symbols correspond to IPN75, IPN 50 and IPN25, respectively.

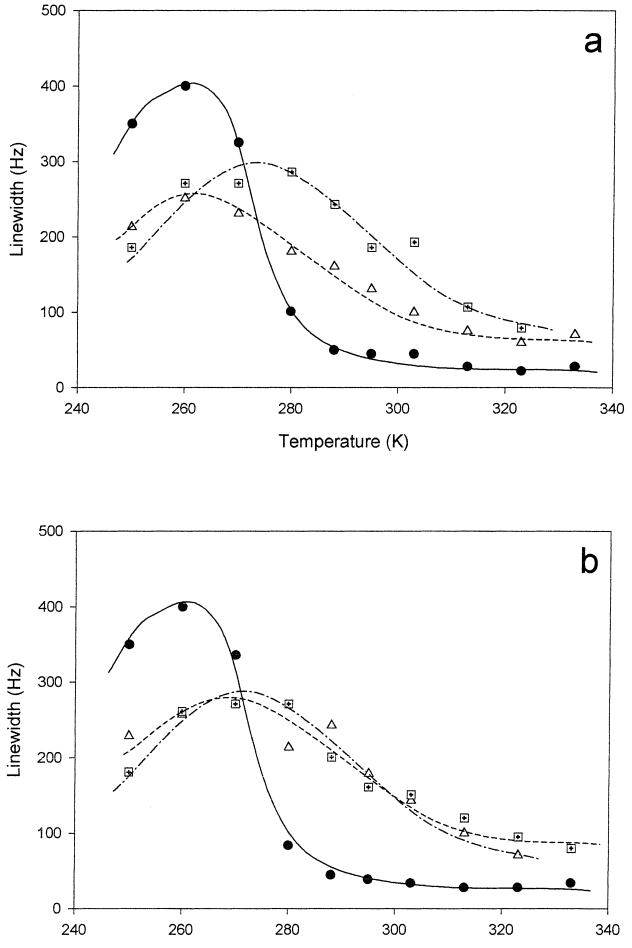

Fig. 3. Temperature dependence of PMPS aromatic carbon line widths of PMPS (● plain line), IPN75 (△ dashed line) and IPN25 (⊞ dashed dotted line); lines are guide for the eye. (a) 127 ppm line; (b) 133 ppm line.

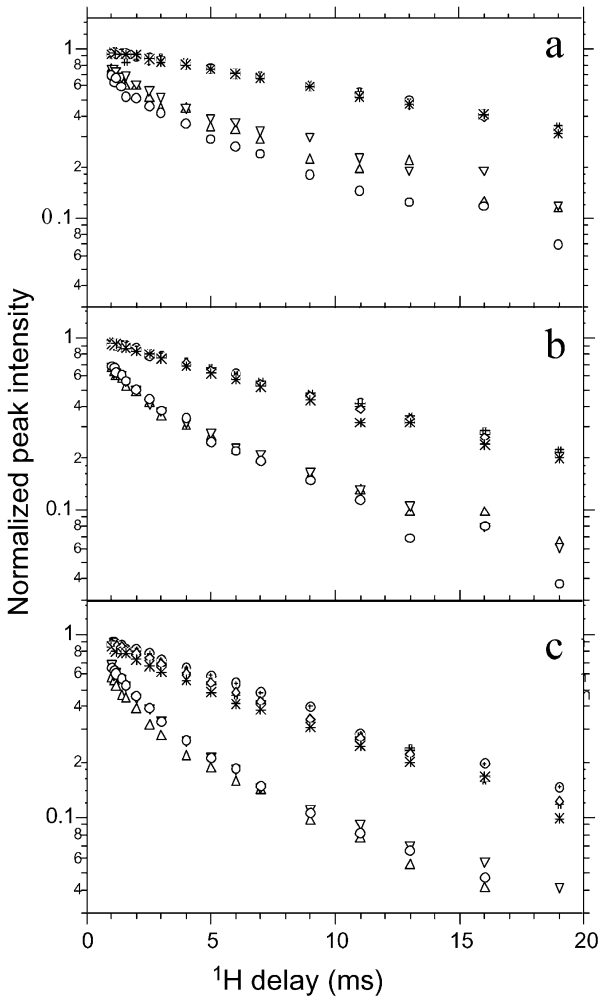

Fig. 4. $T_{1\rho}(^1H)$ decays measured on carbons of the different IPN samples as a function of the delay in the delayed contact time pulse sequence; (a) IPN25, (b) IPN50 and (c) IPN75. PMPS carbons (○, ▽ and △ symbols); PMMA carbons (◇, ∗, ⊕ and # symbols).

$t_{CP} = 0.8$ ms whereas both IPN50 and IPN75 exhibit maximum intensities at $t_{CP} = 1.2$ ms.

Examining line widths as a probe of interchain mixing has already been discussed for other polysiloxane based IPNs by Klein et al. [3,27]. The authors found evidence of mutual interpenetration at the phase boundary by using solution state NMR [3]. Line widths measurements can also be performed as a function of temperature by using high-resolution solid-state NMR to probe the bulk organization of IPNs.

Table 2
^{1}H spin–lattice relaxation times in the rotating frame, $T_{1\rho}(^1H)$, of the samples under study, as measured on ^{13}C NMR spectra by using a spin-lock pulse sequence with a delayed contact time

Sample	$T_{1\rho}(^1H)$ PMMA	First $T_{1\rho}(^1H)$ PMPS	Second $T_{1\rho}(^1H)$ PMPS
PMPS	–	4.6	–
IPN75	8.6	4.2	10
IPN50	10.5	3.3	6.6
IPN25	16.9	2.9	6.6
PMMA	20.5	–	–

Fig. 3 shows the line width temperature dependence of two aromatic PMPS carbon lines in neat PMPS, IPN75 and IPN25.

The aromatic carbon lines undergo a maximum line broadening the temperature position of which is composition dependent. For pure PMPS, this maximum takes place near 260 K while it occurs in the range 270–280 K for the IPNs. Besides, the line broadening is observed on a much larger temperature range in the IPNs than in the neat network. Line broadening mechanisms in amorphous polymers examined under MAS and proton DD may have several origins [28]. Particularly, local motions can have significant effects on line widths when their frequency is of the order of the strength of the ^{1}H decoupling field expressed in frequency units. In the present case, the line broadening observed in the PMPS network is clearly due to the PMPS chain motions associated with the glass transition phenomenon. The line broadening of the PMPS carbon lines in the IPNs has the same origin. However, its dependence as

a function of the IPN composition shows that the PMPS local chain motions are sensitive to the presence of the PMMA units, which supports the interpenetrating character of the networks. The larger temperature range over which the line broadening of the ^{13}C PMPS aromatic lines occurs can be interpreted in terms of a broader distribution of the PMPS unit environments in the IPNs than in the neat network. No line broadening was observed for PMMA in the investigated temperature range indicating that there are no chain motions of the PMMA units in this temperature range.

The $T_{1\rho}(^1H)$ values of the neat PMMA and PMPS homopolymer networks and IPN samples, measured via high-resolution solid-state ^{13}C NMR, are reported in Table 2. In the neat networks, as a result of spin diffusion, all carbons exhibit an exponential $T_{1\rho}(^1H)$ decay characterized by a single $T_{1\rho}(^1H)$ for each homopolymer network. The glassy PMMA network has a much longer $T_{1\rho}(^1H)$ (20.5 ms) than the rubbery PMPS network (4.6 ms).

IPNs show a more complex behavior. As shown in Fig. 4, PMMA carbons and PMPS carbons exhibit different $T_{1\rho}(^1H)$ decays. The PMMA decay has an exponential dependence on time over the time range investigated (20 ms). As shown by data reported in Table 2, the associated $T_{1\rho}(^1H)$ depends on the IPN composition. At low PMPS concentration (IPN25), PMMA $T_{1\rho}(^1H)$ is close to the $T_{1\rho}(^1H)$ of neat PMMA whereas, at high PMPS content (IPN75), the $T_{1\rho}(^1H)$ of the PMMA chains has a much lower value. The existence of an exponential decay over a rather large time range shows that a large amount of PMMA units have a quite well-defined environment in the IPNs. The composition dependence of the $T_{1\rho}(^1H)$ clearly indicates that, within a distance of a few nanometers, PMMA and PMPS units co-exist.

The $T_{1\rho}(^1H)$ decays of the PMPS carbons in the IPNs are not monoexponential. They can be fitted with a sum of two exponential functions, resulting in two $T_{1\rho}(^1H)$ whose values are listed in Table 2. The shorter $T_{1\rho}(^1H)$ value is close to the $T_{1\rho}(^1H)$ of neat PMPS and the longer $T_{1\rho}(^1H)$ is composition dependent. Therefore, as a first approximation, the PMPS chains may be considered to experience two different environments. Some IPN regions are PMPS-rich; other regions correspond to a close interpenetration of PMMA and PMPS units, at the scale of a few nanometers.

4. Conclusion

All the techniques used in the present work give information on the interpenetrating character of the IPNs at different scales. The transparency of the materials shows that the domain sizes in the materials under study are smaller than a few hundreds of nanometers. At the much smaller length scales of a few angstroms or nanometers, all the NMR experiments based on either line width measurements or CP rise show that the IPN behavior is clearly different from the neat network behavior and, therefore, they indicate that the PMPS and PMMA chains are highly interpenetrating. In this respect, CP data are particularly interesting since they probe the close neighborhood of each carbon. However, the description of the network chain organization as deduced from the NMR approach is much more complex: the line width dependence of the PMPS aromatic carbons as a function of temperature demonstrates that the variety of PMPS unit environments is larger in the IPNs than in the PMPS network. More information is derived from the $T_{1\rho}(^1H)$ decays which show that the PMPS chain environment has a bimodal distribution, with PMPS-rich domains where the PMMA presence is barely detected and PMPS/PMMA interpenetrating domains where the PMMA subchains are mostly located. It must be noticed that such a description is in agreement with the DSC analysis of the IPN samples: the onset of the PMPS glass transition is observed at temperatures equal to or only very slightly higher in the IPNs than in the PMPS network, which corroborates the existence of PMPS-rich domains. Besides, the width of the glass transition, as determined from DSC, can be explained in terms of the distribution of PMPS environments involving more and more methyl methacrylate units on increasing temperature.

Finally, it is interesting to note that the PMMA and PMPS chains do not play a symmetric role in the solid-state organization of the network. Within the sensitivity of the NMR experiments, the distribution of PMMA environments appears to be much more narrow than the distribution of PMPS environments. Such differences in behaviors may be related to the glass transition temperatures of the IPN components. Once the IPN is formed, the PMMA subchains do not exhibit chain motions in the temperature range investigated, as shown by the line width measurements. Therefore, they cannot undergo any reorganization at room temperature and are trapped within the network. On the opposite, the PMPS units have a significant mobility, which is reflected by the PMPS line broadening and can lead to a partial reorganization of the sub-chains, with some small PMPS-rich domains with characteristic dimensions of a few nanometers. The possible reorganization of PMPS chains might occur during the last step of synthesis during which the PMMA network is formed. As a matter of fact, this latest polymerization occurs at 70 °C i.e. far above the PMPS T_g. During this step, PMPS chains can reorganize more easily since the PMMA network is not yet formed. This would thus explain the presence of PMPS-rich domains together with interpenetrating domains.

References

[1] Klempner D, Sperling LH. Interpenetrating polymer networks, Advances in Chemistry Series No. 239. Washington: American Chemistry Society, 1994.
[2] Olabisi O, Robeson LM, Shaw MT. Polymer–polymer miscibility. New York: Academic Press, 1979.

[3] Klein PG, Ebdon JR, Hourston DJ. Polymer 1988;29:1079–85.
[4] Caille JR, Teyssié D, Bouteiller L, Bischoff R, Boileau S. Macromol Symp 2000;153:161–6.
[5] Song M, Hourston DJ, Schafer FU, Pollock HM, Hammiche A. Thermochim Acta 1998;315:25–32.
[6] Vatalis AS, Delides CG, Georgoussis G, Kyritsis A, Grigorieva OP, Sergeeva LM, Brovko AA, Zimich ON, Shtompel VI, Neagu E, Pissis P. Thermochim Acta 2001;371:87–93.
[7] Utracki LA. Polymer alloys and blends. Munich: Hanser, 1989.
[8] Kaplan DS. J Appl Polym Sci 1976;20:2615–29.
[9] Clarson SJ, Semlyem JA, Dogson K. Polymer 1991;32:2823.
[10] Frisch HL, Zhou P. Phase morphology of simultaneous IPNs. Effects of differences of component solubility parameters and glass-transition temperatures. In: Klempner D, Sperling LH, Utracki LA, editors. Interpenetrating polymer networks, Advances in Chemistry Series, vol. 239. Washington, DC: ACS, 1994. p. 269.
[11] Stern SA, Shah VM, Hardy BJ. J Polym Sci Part B: Polym Phys 1987;25:1263–98.
[12] Tonelli AE. High resolution solid-state NMR studies of polymer chemical and physical structures. In: Ibett RN, editor. NMR spectroscopy of polymers. London: Blackie Academic and Professional, 1993. p. 161–97.
[13] Lauprêtre F. NMR basic principles and progress, vol. 30. Berlin: Springer, 1994 p. 65–109.
[14] Lau C, Zheng S, Zhong Z, Mi Y. Macromolecules 1998;31:7291–7.
[15] McBrierty VJ, Packer KJ. Nuclear magnetic resonance in solid polymers. Cambridge: Cambridge University Press, 1993.
[16] Stejskal EO, Schaefer J, Sefcik MD, Mckay R. Macromolecules 1981;14:275–9.
[17] Caravatti P, Deli JA, Bodenhausen G, Ernst RR. J Am Chem Soc 1982;104:5506–7.
[18] Cheung MK, Wang J, Zheng S, Mi Y. Polymer 2000;41:1469–74.
[19] Schmidt-Rohr K, Clauss J, Spiess HW. Macromolecules 1992;25:3273–7.
[20] Schmidt-Rohr K, Clauss J, Blümich B, Spiess HW. Magn Reson Chem 1990;28:S3–S9.
[21] da Silva NM, Tavares MIB, Stejskal EO. Macromolecules 2000;33:115–9.
[22] Wang J, Cheung MK, Mi Y. Polymer 2001;42:3087–93.
[23] Perera MCS, Ishiaku US, Ishak ZAM. Eur Polym J 2001;37:167–78.
[24] Szeverenyi NM, Sullivan MJ, Maciel GE. J Magn Reson 1982;47:462–75.
[25] Caille JR. PhD Thesis, Université Paris VI, 1997.
[26] Stejskal EO, Schaefer J, Mc Kay RA. J Magn Reson 1977;25:569–73.
[27] Ebdon JR, Hourston DJ, Klein PG. Polymer 1984;25:1633.
[28] VanderHart DL, Earl WL, Garroway AN. J Magn Reson 1981;44:361–401.